



MINISTRY OF TECHNOLOGY

AERONAUTICAL RESEARCH COUNCIL

CURRENT PAPERS

Low - Speed Characteristics  
of Waverider Wings

by

*R. F. A. Keating*

*B. L. Mayne*

*Aerodynamics Dept., R.A.E., Bedford*

LONDON: HER MAJESTY'S STATIONERY OFFICE

1970

PRICE 9s 0d [45p] NET



U.D.C. 533.692.55 : 532.527 : 533.6.011.32

LOW-SPEED CHARACTERISTICS OF WAVERIDER WINGS

by

R. F. A. Keating

B. L. Mayne

SUMMARY

This paper reports on low-speed wind tunnel studies of a series of simple delta-like shapes which might form the basis of future hypersonic aircraft.

The nature of the vortices formed above these wings was investigated by oil-flow experiments, smoke visualisation and flow surveys. Some of the vortices could only be described as broken and had a stagnation point at the centre. Nevertheless, the vortices still had a strong circulation and a high static suction.

The force characteristics were typical of current slender wing designs in spite of the anomalous vortices. The large shift of the aerodynamic centres of the hyperbolic planforms when changing from hypersonic to low-speed flight may prove embarrassing.

CONTENTS

	<u>Page</u>
1 INTRODUCTION	3
2 MODEL GEOMETRY AND EXPERIMENTAL DETAILS	3
3 NATURE OF THE FLOW	5
4 LONGITUDINAL CHARACTERISTICS	6
5 LATERAL CHARACTERISTICS	6
6 CONCLUSIONS	7
Table 1 Model planform geometry	8
Table 2 Planforms of waverider wings	9
References	10
Illustrations	Figures 1-21
Detachable abstract cards	-

## 1 INTRODUCTION

Hypersonic waverider aircraft<sup>1</sup> show considerable promise of providing really long ranges in the future<sup>2</sup>. However one of the characteristics which may prove crucial in the design is the large shift of the aerodynamic centre when changing from hypersonic to subsonic flight. A series of models was designed to provide some guidance on the limitations imposed by considerations of low-speed performance on the choice of cone-flow waverider planform shapes from the inherently large range possible.

Present thoughts are in terms of delta-like shapes for all the waverider types, with basically sharp leading edges. Cruise considerations dictate values of slenderness ratio,  $s/l = \text{semispan/length}$ , between 0.2 and 0.3, which is not too small for satisfactory low-speed qualities and is in the order of slenderness of current supersonic transport designs. The models used in the present investigation were designed at a time when it was thought that the nose might have to be blunted, in an attempt to investigate the effect of planform nose shape on wings of constant slenderness. The models are simplified forms of waverider wings having plane under-surfaces, triangular cross-sections and a blunt base for a trailing edge. A single, fully representative model of a waverider with camber and thickness distribution obtained from conical shock and expansion theory<sup>3</sup> completed the series.

The tests involved six-component force measurements, as well as oil-flow and smoke flow visualisation tests aimed at establishing the nature of the separated flow field. Studies were made of the velocity distribution through the vortex cores on some of the wings, in particular to establish the nature of an unusual 'vortex-breakdown' demonstrated by smoke on the more blunt-nose planforms.

The tests were performed in the 13ft x 9ft low-speed wind tunnel at R.A.E. Bedford during 1965 and 1966.

## 2 MODEL GEOMETRY AND EXPERIMENTAL DETAILS

Figs.1 and 2 show the planform shape and thickness distribution respectively of the wing models and Tables 1 and 2 give numerical details of the planforms. Models A and B were intended as reference models to relate the results of the current tests with flat plate results and are simple deltas having leading edge sweeps of 65° and 70°. The remainder of the series have the same slenderness as the 65° delta and differ only in planform shape

(Models C, D and E have zero sweep at the nose which increases to  $67.5^\circ$ ,  $70^\circ$  and  $72.5^\circ$  respectively at the trailing edge; models H, G and F have constant sweep at the trailing edge of  $70^\circ$  with a pointed apex of sweeps  $20^\circ$ ,  $40^\circ$  and  $60^\circ$  respectively. The equations of the segments used to define the planform are conics (the intersection of a plane with a cone) of the form:-

$$y^2 + Py + Qx + Rx^2 = 0 \quad .$$

Numerical values of P, Q and R are listed in Table 1. The cross sections of this series of models are triangular with a plane underside, a triangular base at the trailing edge and sharp leading edges. Real waveriders will differ from this geometry, but it is expected that the leading edge would be of small radius and the exit of the engine (jet or rocket) would be large and not running full at low speeds.

Fig.3 shows the fully representative model of a cone-flow designed waverider wing. It should be noted that the fin arises automatically from the concepts used in designing the upper surface and apart from a slope discontinuity on the upper surface the wing can quite definitely be regarded as a slender wing at low speeds.

Six-component force measurements were made and these were reduced to coefficient form in stability axes system using the planform area, root chord and span as the reference dimensions. The reference centre was arbitrarily chosen as the centroid of the cross section at  $50\%$  root chord from the apex for the series of wings and at  $50\%$  root chord along the ridge line on the cone-flow design.

Oil flow experiments using the method of Ref.4 were made on all the wings to investigate the nature and stability of the flow. Examples are shown in Fig.4 for wing D and for various wings in Fig.5. The nature of the vortices at low incidences was investigated on wing E and the results are shown in Fig.6.

The nature of the vortex on wing D at an incidence of  $16^\circ$  was investigated by a five-tube pitot-static yawmeter probe. Velocity surveys of the flow were made in a plane normal to the wind at  $40\%$  root chord, presented in Fig.14, and in vertical traverses through the vortex centres at  $2\%$ ,  $10\%$ ,  $20\%$ ,  $40\%$  and  $70\%$  root chord, presented in Figs.12 to 14. A vertical traverse was

also made on Wing A at 40% root chord and similar flat plate delta wing for the purposes of comparison.

Smoke injected at the apex of the wing, in the manner of Ref.5, was used in order to measure the position of vortex breakdown and to reveal the character of the vortex. This technique was also used as an adjunct to the velocity surveys to ensure that the traverse gear did not greatly disturb the vortex and that the smoke did not disturb the vortex.

### 3 NATURE OF THE FLOW

Figs.4 and 5 show typical surface flow patterns on various waverider wings some of which can be classified as slender in shape and behaviour. The patterns show that the vortex system at large angles of incidence, when  $\alpha$  is greater than the base angle, is unified. Changes in incidence do not change the form of the system, but alter the strength and to some extent the position of the vortex. In particular the true horseshoe vortex of the Norman wings is most gratifying when, a priori, a mixed flow of a bubble and part-span vortices may have been expected.

However at low angles of incidence when the vortices are weak the 'Norman' wings have part-span vortices as shown by the examples in Fig.6. It is expected that the distribution of thickness would have a significant effect at these incidences which are within the angle subtended by the base at the apex.

An interesting aspect of the 'Norman' wings is the nature and early occurrence of vortex breakdown. Smoke injected near the apex gives an indication of the character of the wing vortices and some examples are shown in Fig.7. Normally when smoke is injected into the apex of a slender wing the smoke remains in a tubular region surrounding the vortex core<sup>5</sup>; vortex breakdown is indicated by the diffusion and spread of smoke away from the tube as in Fig.7. In the 'Norman' wings the smoke tube was absent at zero sideslip and a 'woolly' diffuse collection of smoke existed in the whole of the vortex. Analyses of the position of vortex breakdown at large angles of sideslip, such as Figs.8 and 9, show that at zero sideslip the vortex has a broken or conjugate state over the whole of the vortex.

Further support for this contention is shown by the flow studies on wing D at zero sideslip in a transverse plane and in vertical traverses through the centre of the vortex. The results, plotted in Figs.10 to 14,

demonstrate unusually low kinetic pressures and total heads in a large region in the middle of the vortex. The profiles Figs.10 to 13, have a remarkably similar shape at all points along the vortex line, that is, a unified vortex development.

Because of the possibility of the traverse gear disturbing the vortex a comparison of kinetic pressure profiles of three wings is shown in Fig.14. This figure suggests that the gear does not upset the vortex and that the vortex on wing D could be regarded as having an abnormally large vortex core.

#### 4 LONGITUDINAL CHARACTERISTICS

The lift and pitch curves shown in Figs.15 and 16, are very similar to those found on current slender wing aircraft designs both in magnitude and form. Delta wing A provides a typical illustration of the effect of vortex breakdown, above an incidence of  $20^\circ$  there is a loss of non-linear lift at the trailing edge resulting in a marked reduction of lift curve slope and longitudinal static stability (pitch-up). It is remarkable that no other wing of this series shows these characteristics although it is known that the vortices are 'broken' within the range of the measurements.

Fig.17 correlates the aerodynamic centres at  $C_L = 0$  and  $C_L = 0.5$  with the centre of area in the manner first suggested by G.H. Lee. This type of analysis works well for slender wings of ogee delta and gothic planform, and works equally well for the waveriders. The problem of balancing these waveriders is a difficult one, since the high-speed aerodynamic centre is approximately at the centre of area which is rearward of the low-speed centres.

#### 5 LATERAL CHARACTERISTICS

Except for the delta wing A the lateral behaviour of the simplified series of waverider wings are all similar to the 'Norman' wing D. The variations of rolling moment and yawing moment coefficients with side-slip for wing D are shown in Fig.18. In spite of all the doubts about the formation of full vortices at low incidences and the 'broken' vortex at high incidences the characteristics are very close to linear.

The later cone-flow design of waverider is closer to current slender wing designs, but in this case the lateral characteristics are non-linear (Fig.19). The non-linearities are caused by vortex breakdown, which occurs at values of incidences and sideslip expected of a conventional slender wing. The



derivatives for the cone-flow design, Fig.21, are dependent on whether a mean or a slope is used because of the non-linearity but comparison with Fig.20 shows the different behaviour with change in incidence from that of wing D.

Stability and fin effectiveness of all the wings tested are quite adequate to judge by current slender wing designs and would not present a designer with any abnormal problems, except for vortex breakdown occurring on wings approaching current slender wing planforms.

## 6 CONCLUSIONS

The low-speed characteristics of waverider wings of the type considered should not present any more difficulties to the designer than those of current slender wing designs.

The horseshoe shaped vortex flow over the waverider wings with round-nosed planforms has the very diffuse core of a 'broken' vortex yet still has a strong circulation and a large static suction. This vortex flow is worthy of more study from a theoretical and experimental standpoint.

Table 1

MODEL PLANFORM GEOMETRY

Planform co-ordinates were obtained from equation of the form:

$$y^2 + Py + Qx + Rx^2 = 0$$

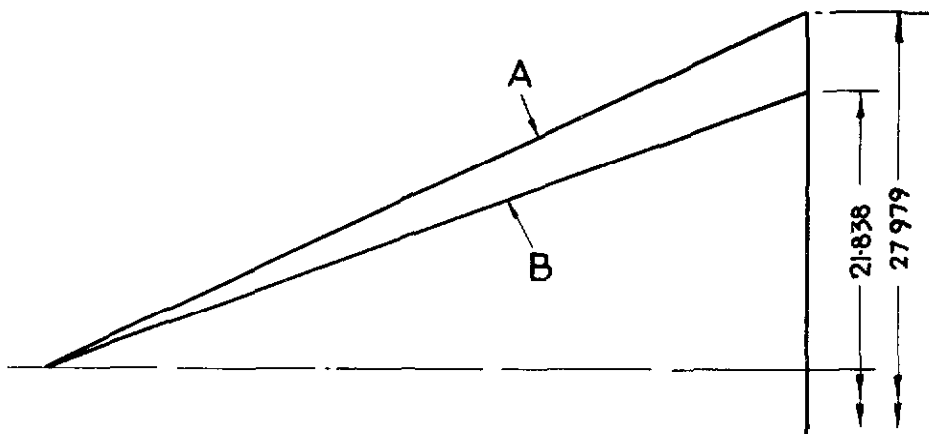
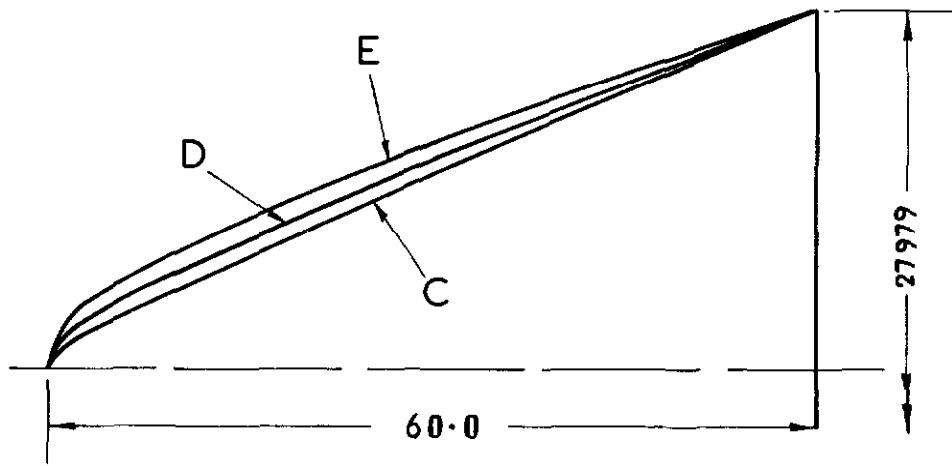
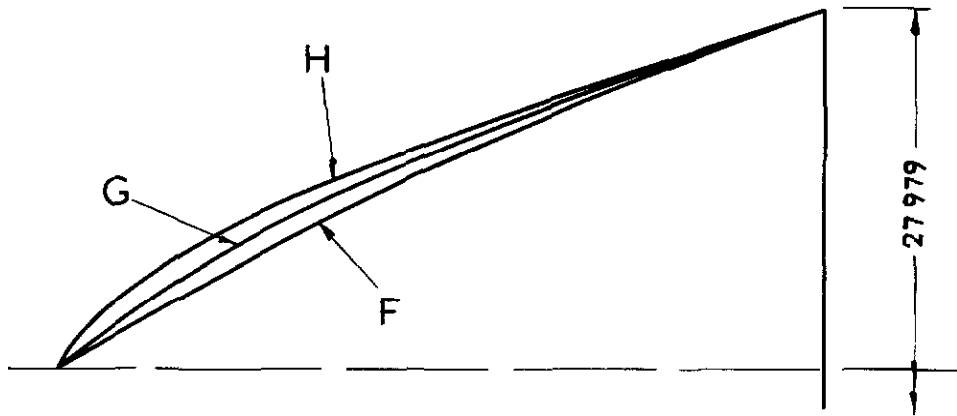
where  $x$  is measured along the centre-line from the nose and  $y$  is measured perpendicular to the centre-line.

Model	$s/l$	Leading-edge sweep at nose	Leading-edge radius at nose	Leading-edge sweep at tail	P	Q	R
A	0.4663		65° DELTA				
B	0.3640		70° DELTA				
C	0.4663	0	1.358 in	67.5°	0	-0.4860	-0.16885
D	"	0	2.862 in	70°	0	-0.9545	-0.12200
E	"	0	4.224 in	72.5°	0	-1.4084	-0.07661
F	"	60°	-	70°	+0.43808	-1.2036	-0.11752
G	"	40°	-	70°	+1.53186	-1.82559	-0.10632
H	"	20°	-	70°	109.71264	-63.34259	+1.00080



REFERENCES

- | <u>No.</u> | <u>Author</u>                                   |   |
|------------|---|---|
| 1          | J. G. Jones                                     | The design of compression surfaces for high supersonic speeds using conical flow fields.<br>A.R.C. R & M 3539 (1963)                            |
| 2          | D. Küchemann                                    | Hypersonic aircraft and their aerodynamic problems.<br>Progress in Aeronautical Sciences, Vol.6, 271-354.<br>Pergamon Press (1965)              |
| 3          | J.G. Jones<br>K.C. Moore<br>J. Pike<br>P.L. Roe | A method for designing lifting configurations for high supersonic speeds, moving axisymmetric flow fields.<br>Ing. Archiv <u>37</u> , 56 (1968) |
| 4          | R.L. Maltby<br>R.F.A. Keating                   | Flow visualisation in low-speed wind tunnels: current British practice.<br>R.A.E. Technical Note 2715 (A.R.C.22373) (1960)                      |
| 5          | R.L. Maltby<br>P.B. Engler<br>R.F.A. Keating    | Some exploratory measurements of leading-edge vortex positions on a delta wing oscillating in heave.<br>A.R.C. R & M 3410 (1963)                |



Dimensions in inches

Fig.1 Wave - rider wing planforms

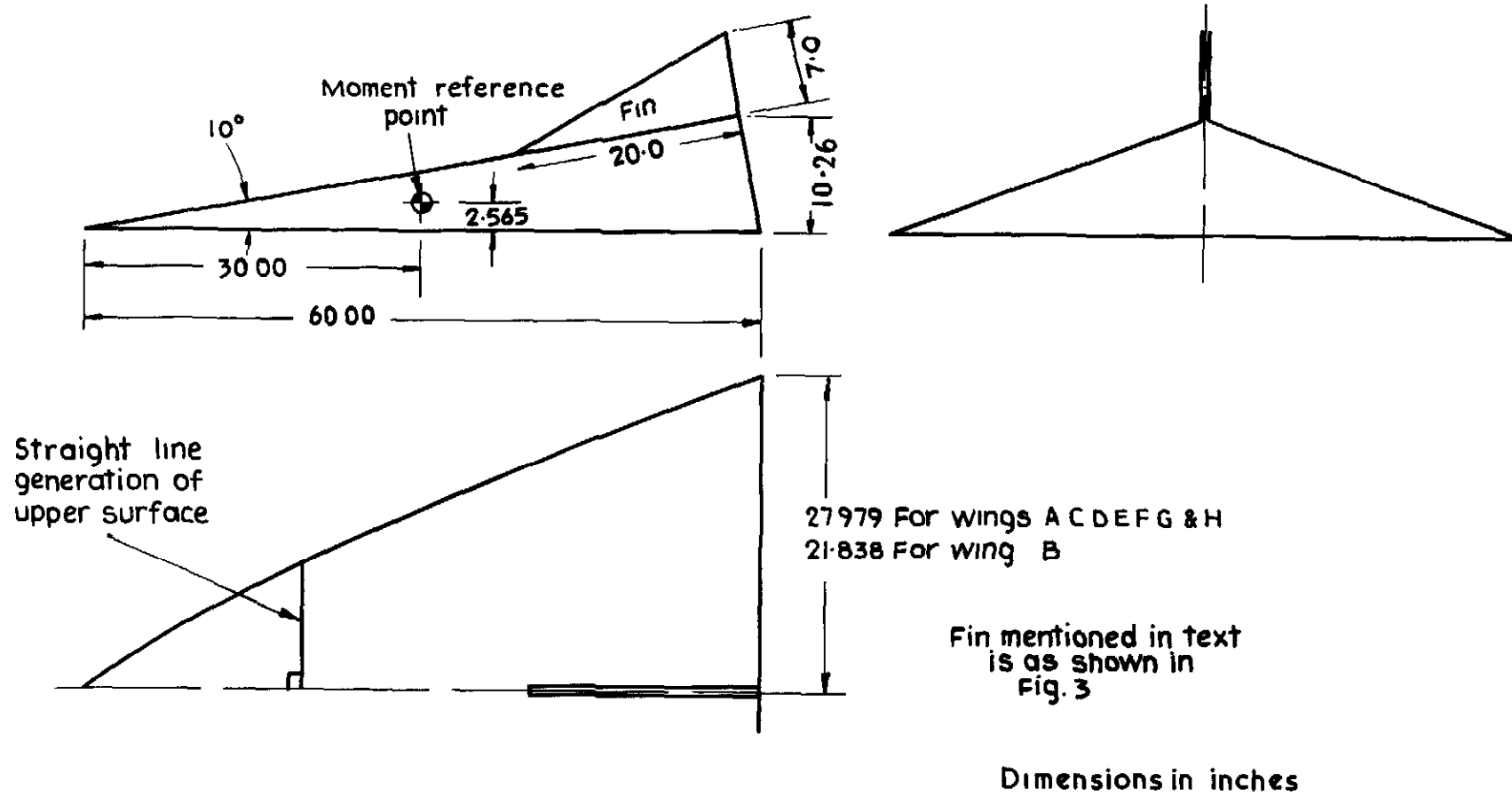


Fig.2 Model geometry

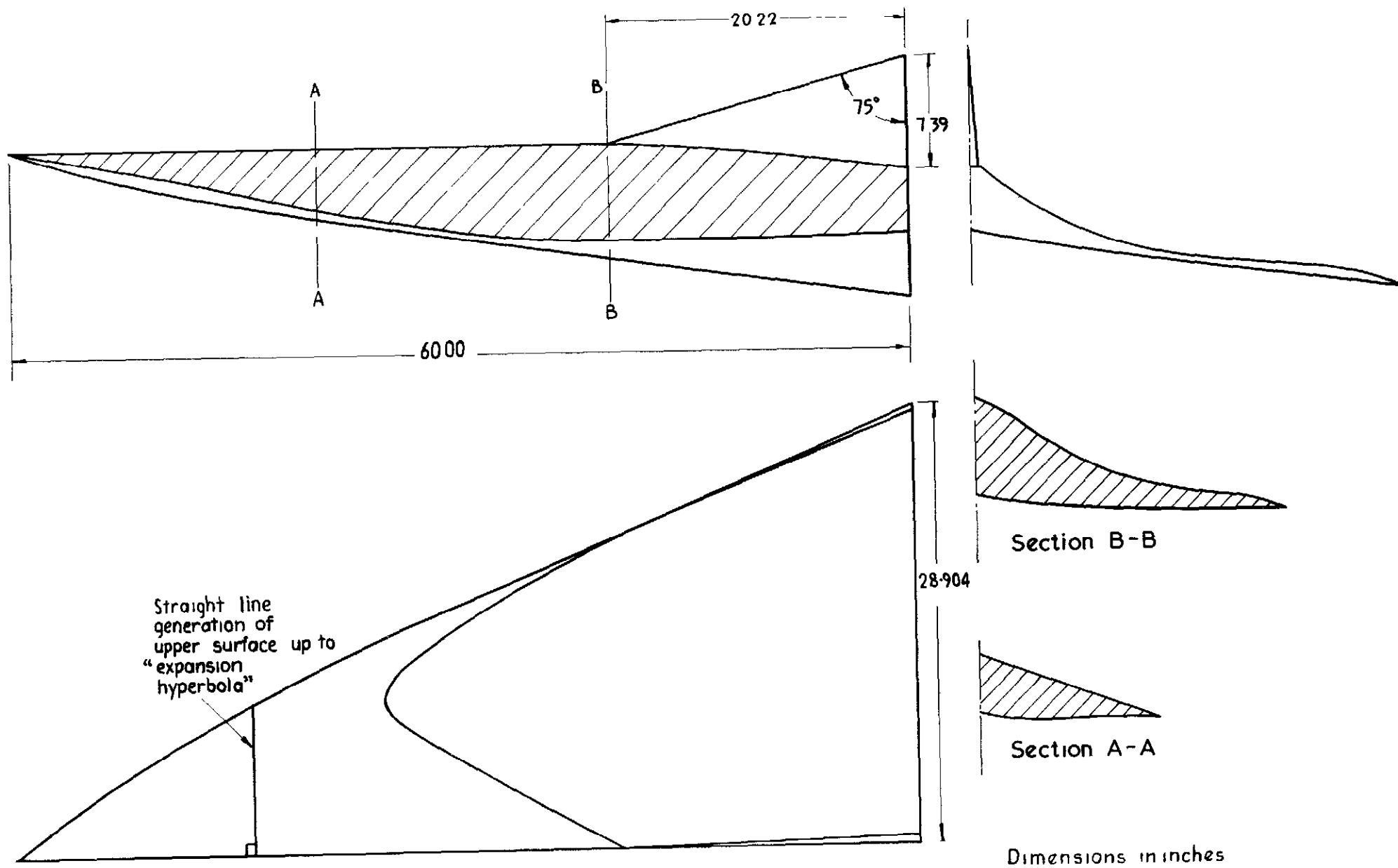
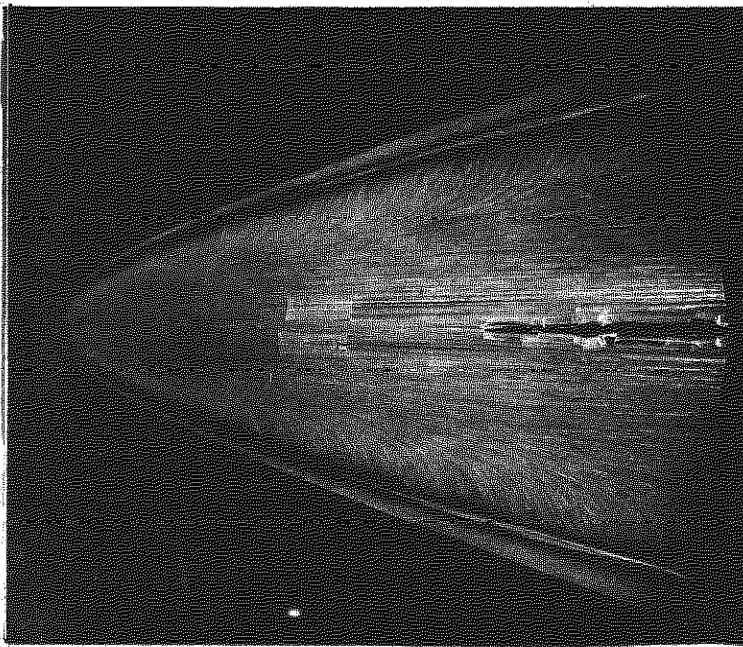
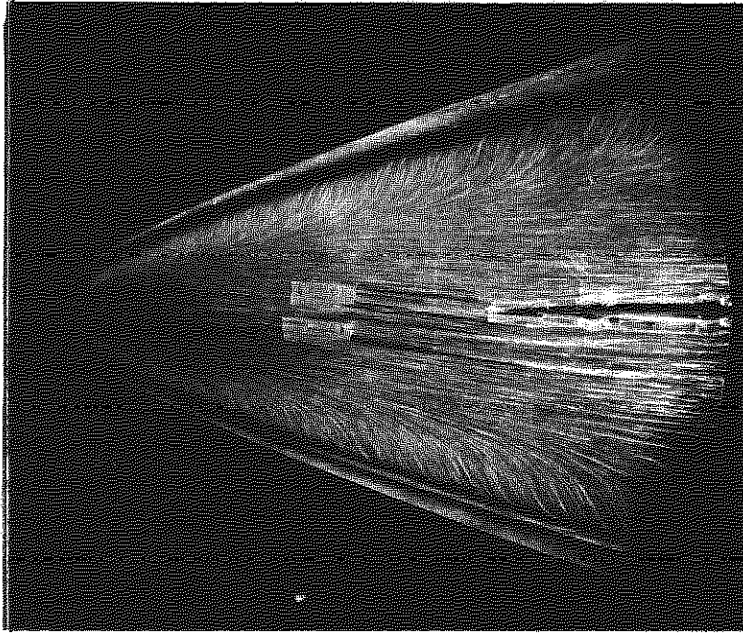


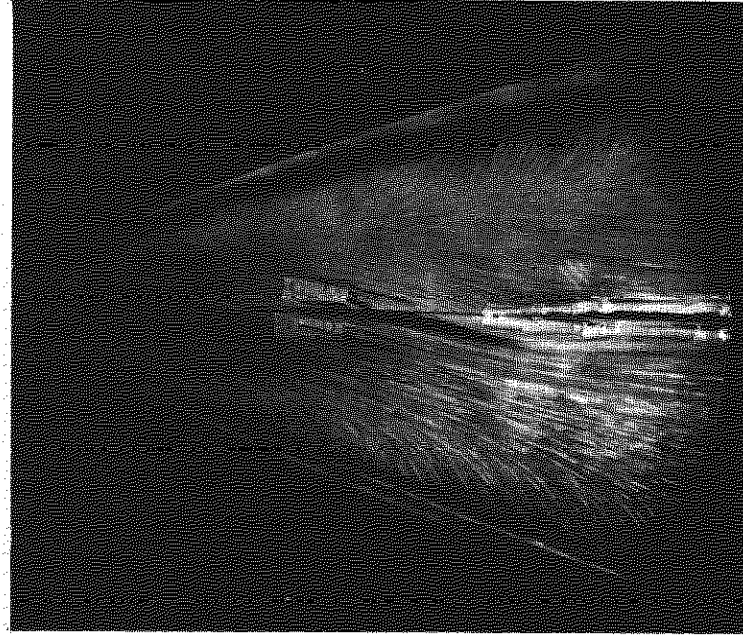
Fig. 3 Cone-flow wave-rider wing model



$\alpha = 16^\circ, \beta = 0^\circ$



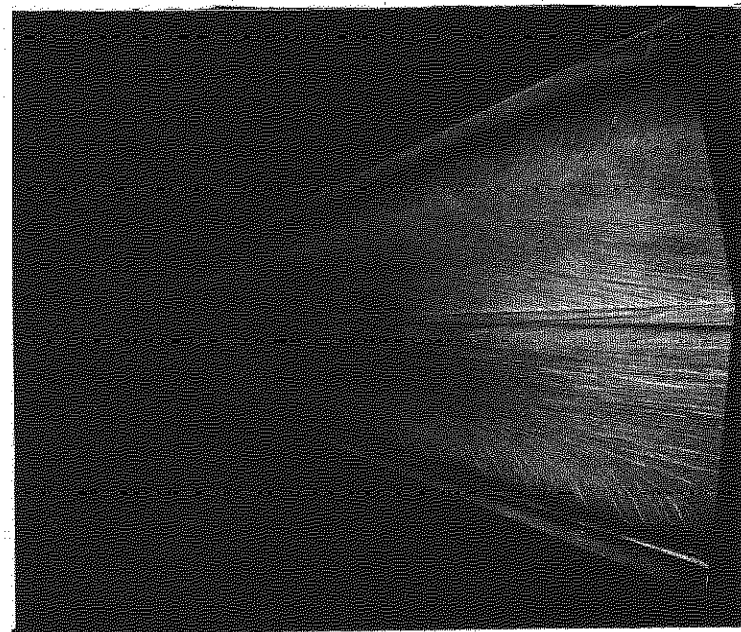
$\alpha = 16^\circ, \beta = 4^\circ$



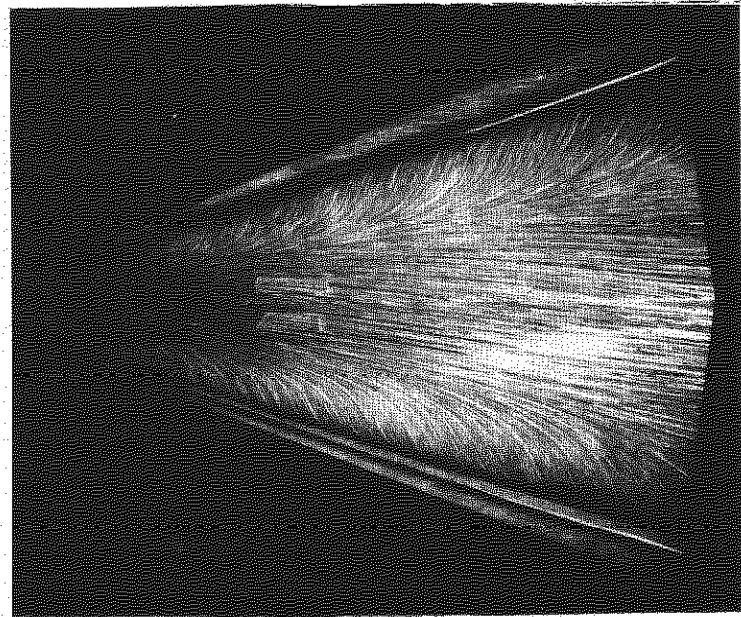
$\alpha = 16^\circ, \beta = 8^\circ$

**Fig.4. Upper surface flow patterns of wing D at high incidences**

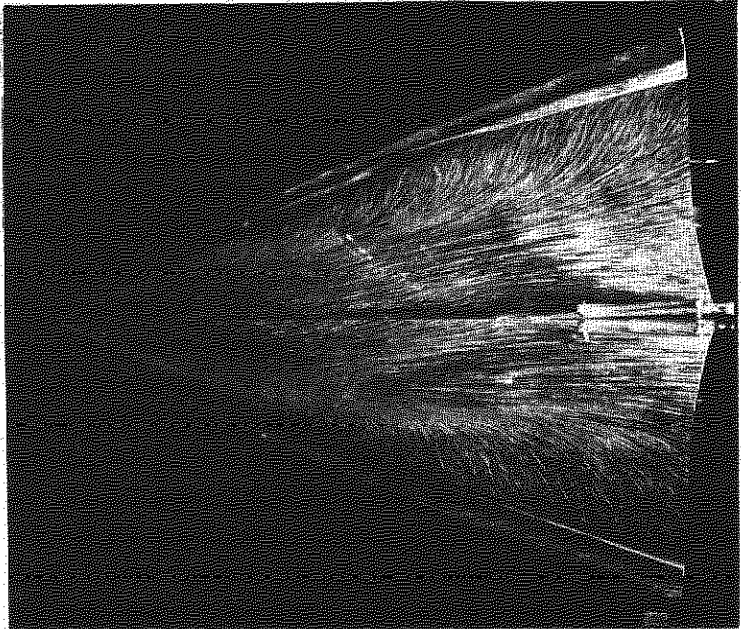




Wing A  $\alpha = 16.8^\circ$ ,  $\beta = 8^\circ$

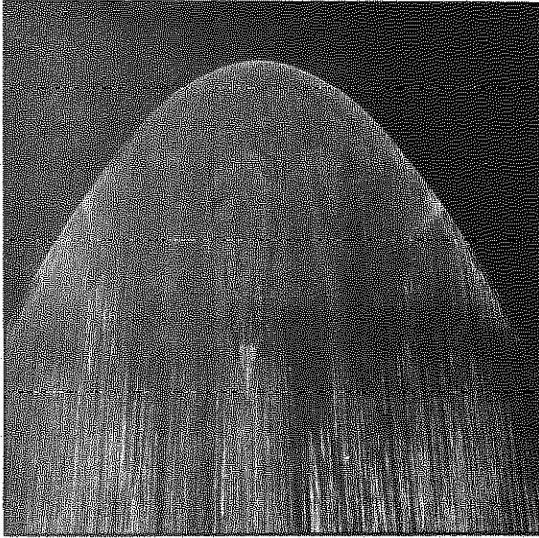


Wing G  $\alpha = 21^\circ$ ,  $\beta = 4^\circ$



Cone-flow wave rider  
 $\alpha = 12.4^\circ$ ,  $\beta = -5^\circ$

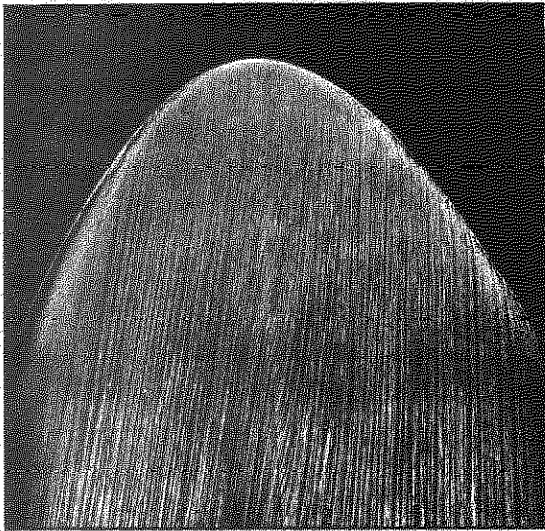
Fig.5. Typical surface flow patterns on wave-rider wings at high incidences and at side-slip



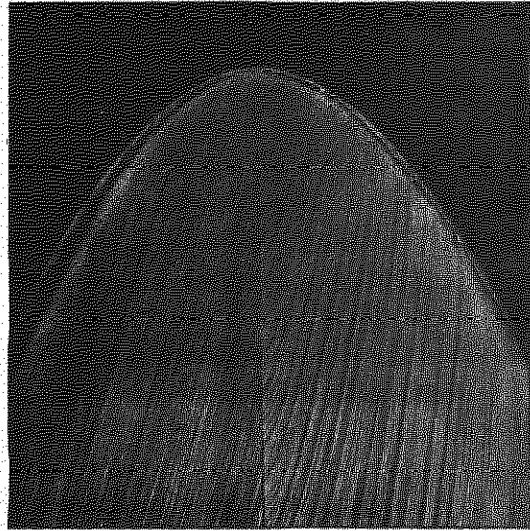
$\alpha = 4^\circ, \beta = 0^\circ$



$\alpha = 5^\circ, \beta = 0^\circ$

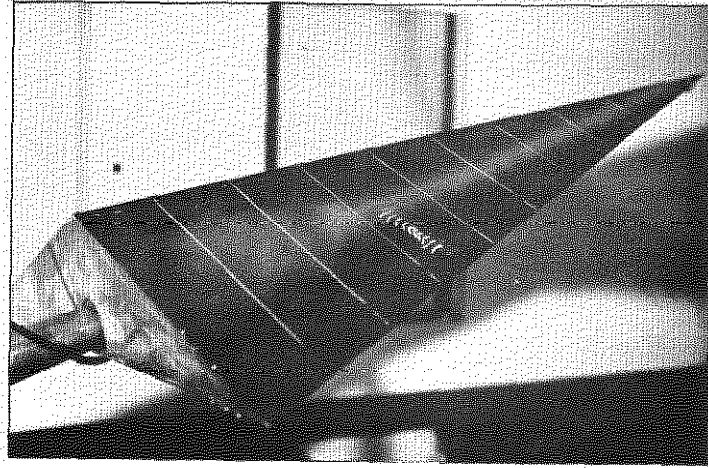


$\alpha = 5^\circ, \beta = 8^\circ$

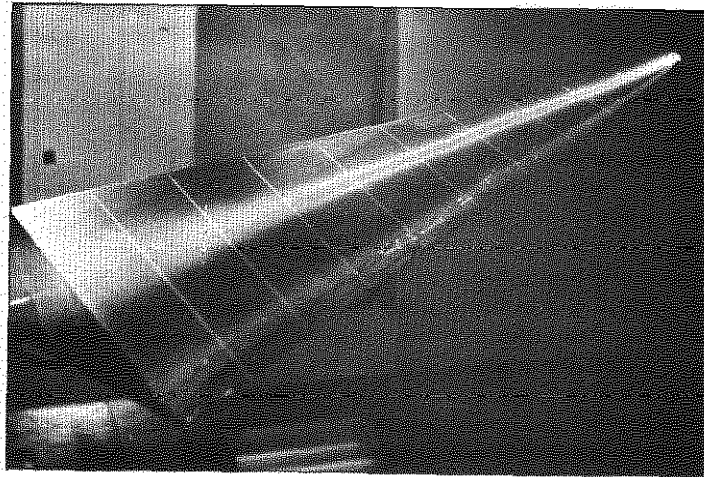


$\alpha = 6^\circ, \beta = 12^\circ$

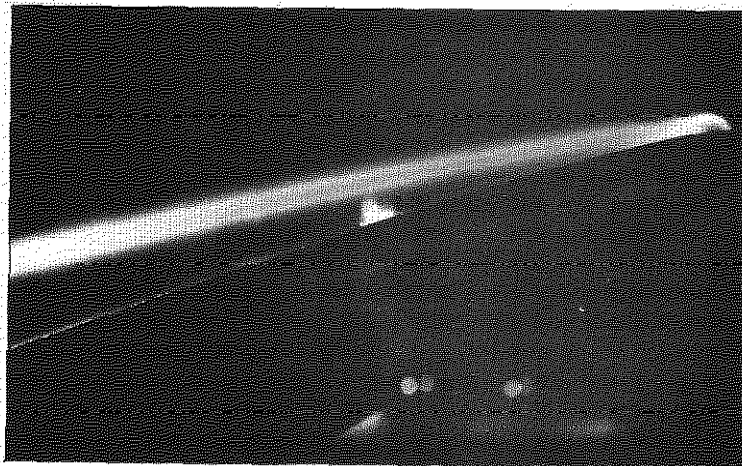
**Fig.6. Upper surface flow patterns of wing E,  
effect of side-slip at low incidences**



Wing A  $\alpha = 23.2^\circ$ ,  $\beta = 0^\circ$ , (Flash photo)



Wing C  $\alpha = 23.2^\circ$ ,  $\beta = 5^\circ$



Wing E  $\alpha = 21.0^\circ$ ,  $\beta = 10^\circ$

**Fig.7. Smoke visualisation of vortices on wave-rider wings.**

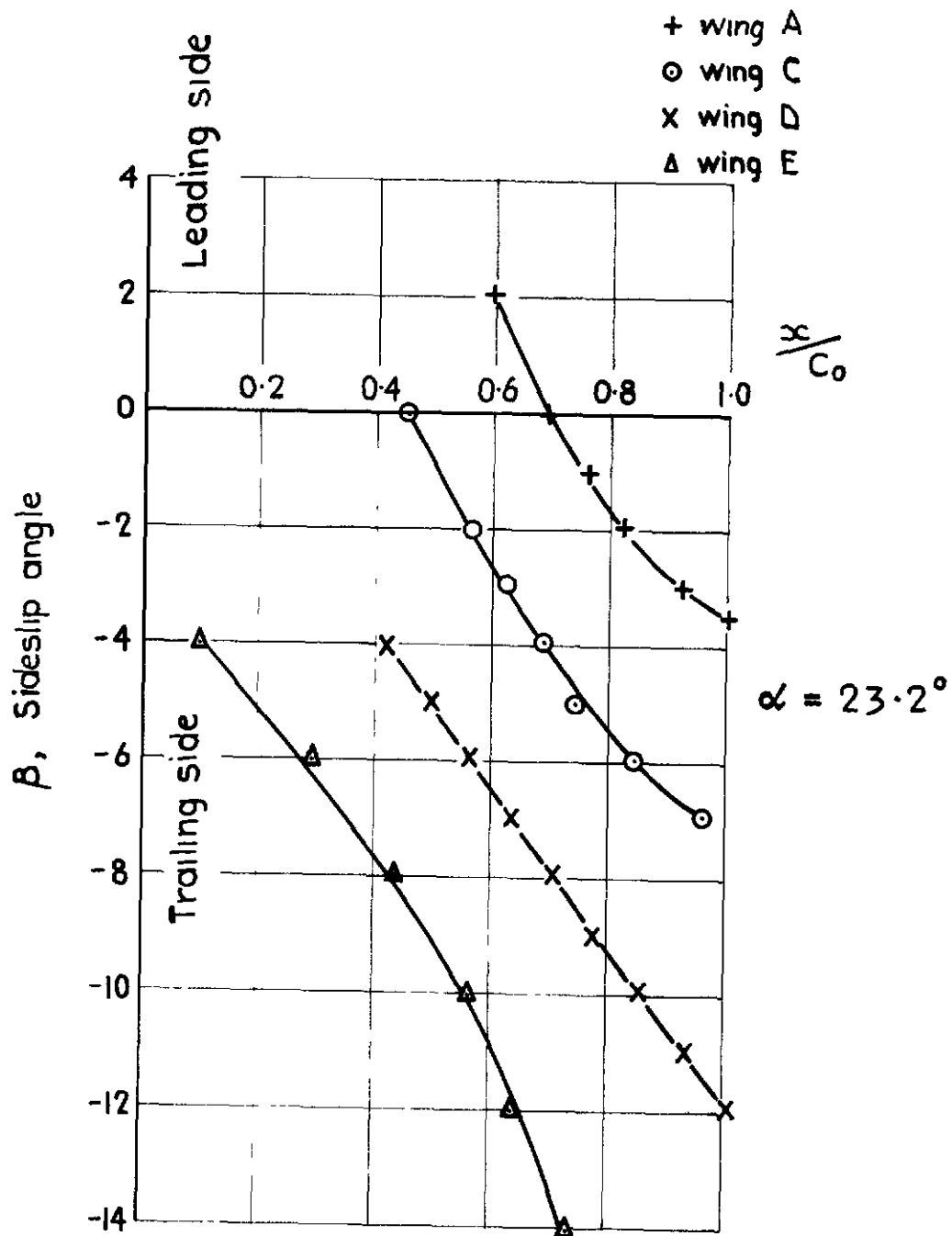


Fig.8 Position of vortex breakdown on normal wings

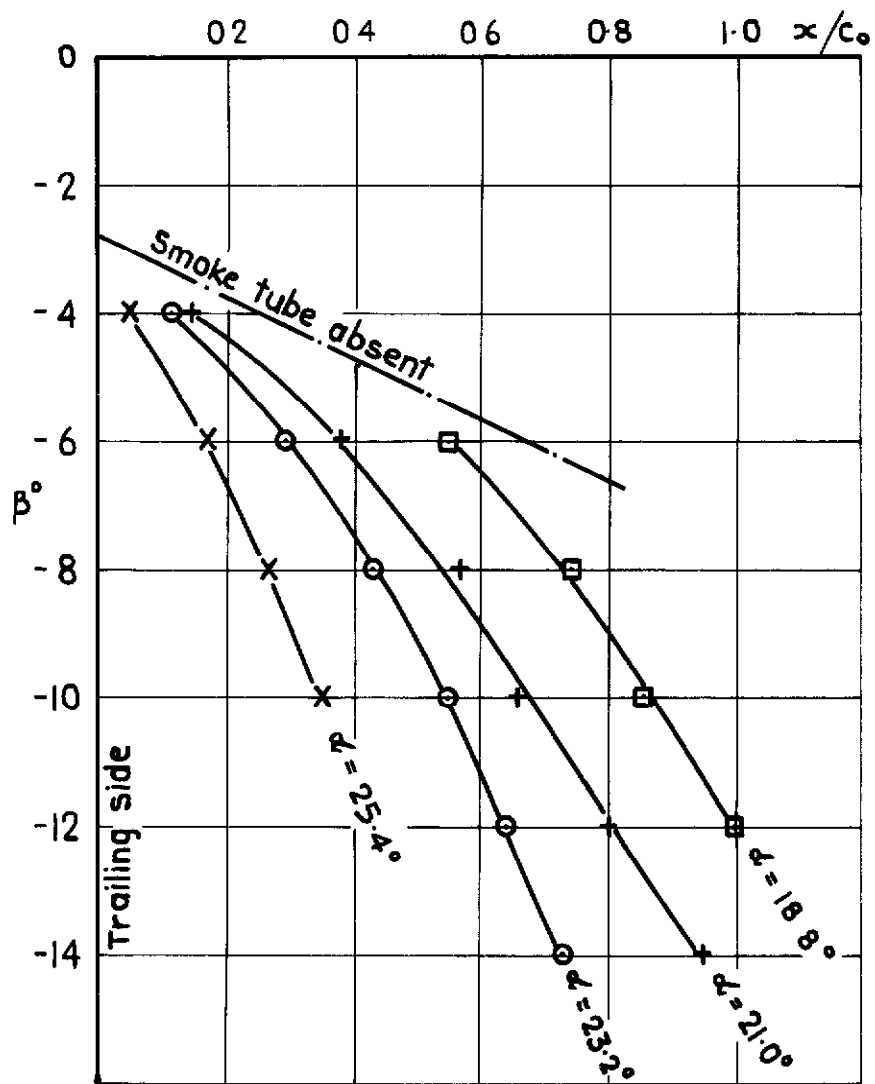


Fig.9 Position of vortex breakdown on wing D

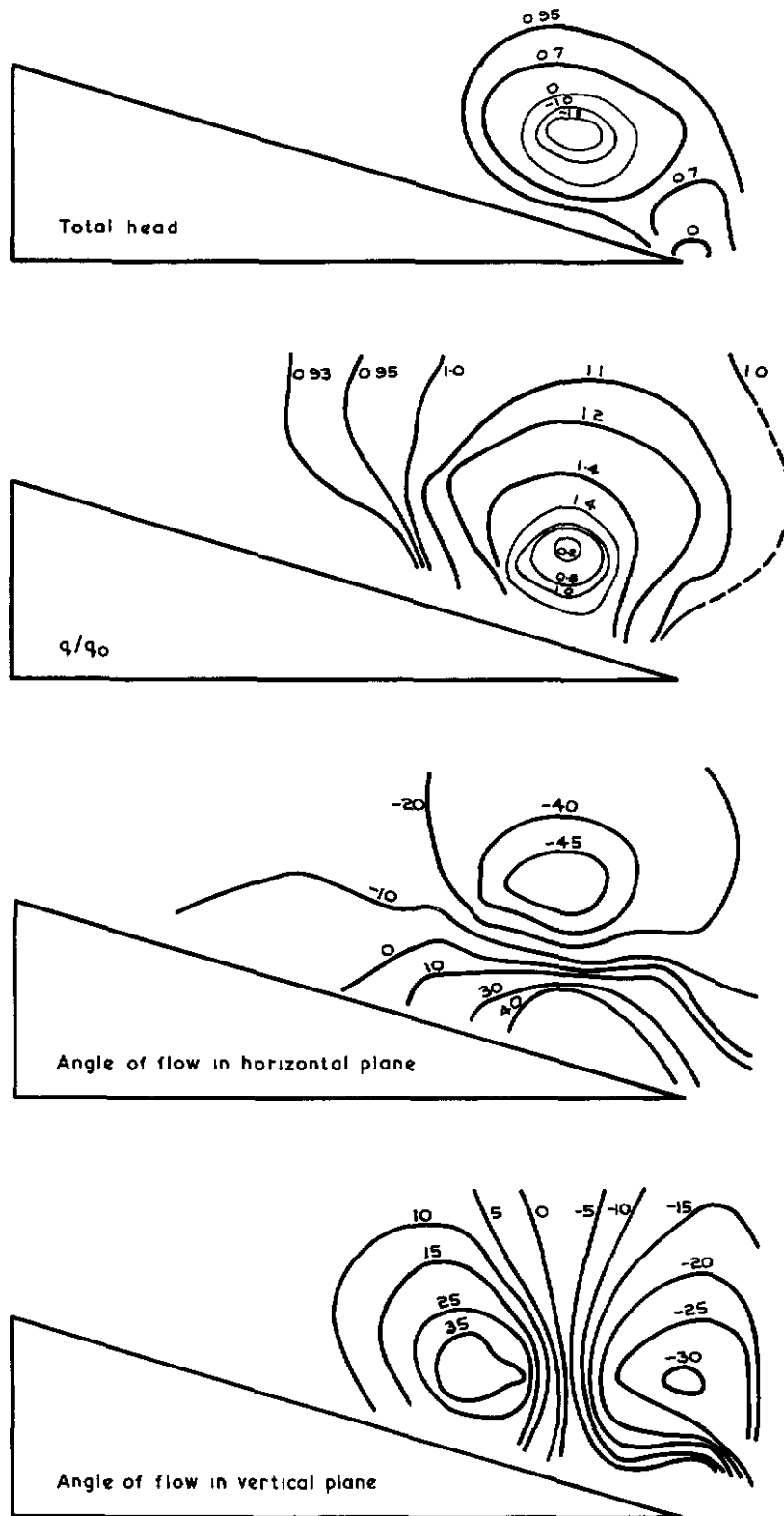


Fig. 10 Flow contours on wing 'D' in a plane at  $40\%$  root chord,  $\alpha = 16^\circ$

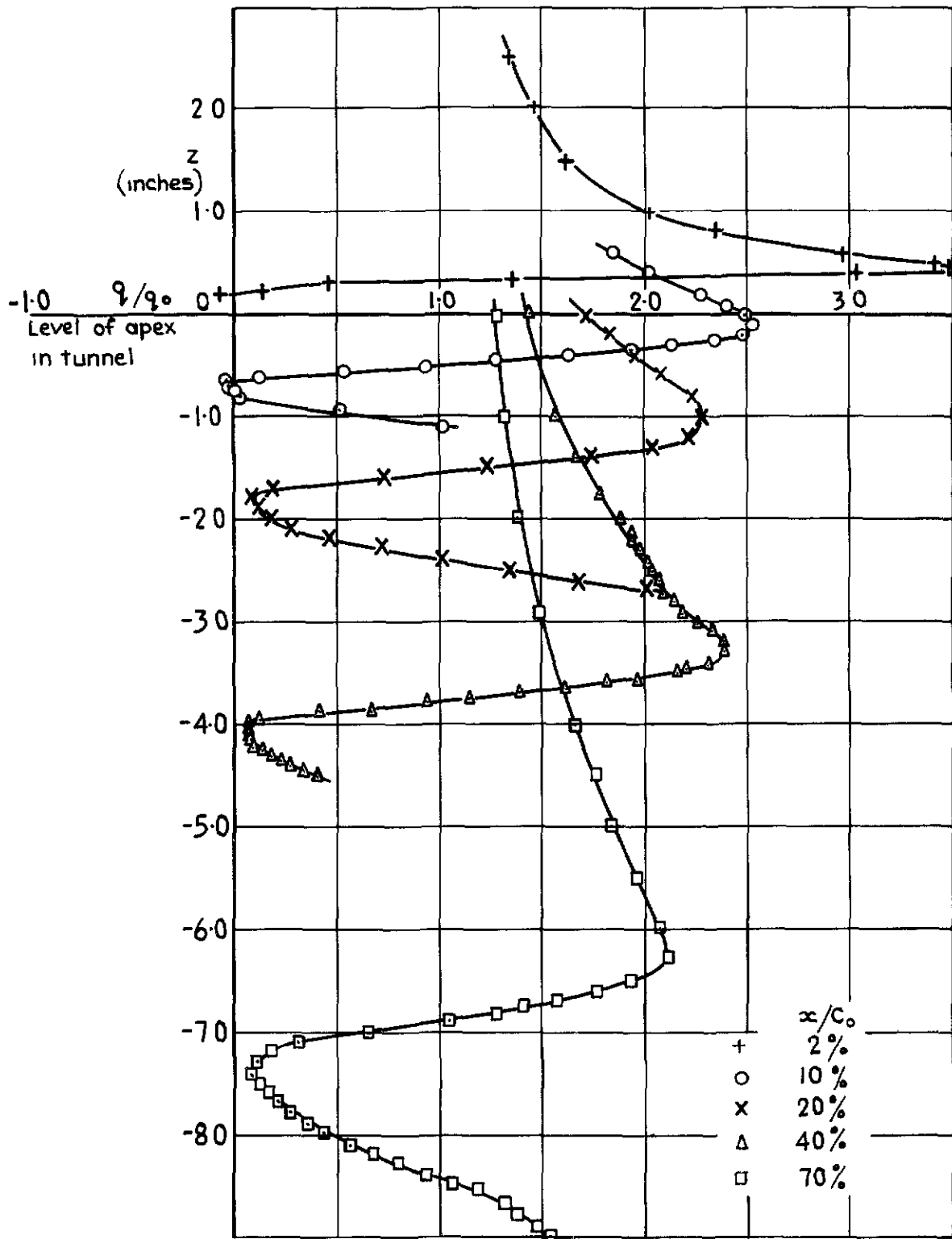


Fig. II 'q' profiles in vertical traverses through vortex centres of wing D at  $\alpha = 16^\circ$

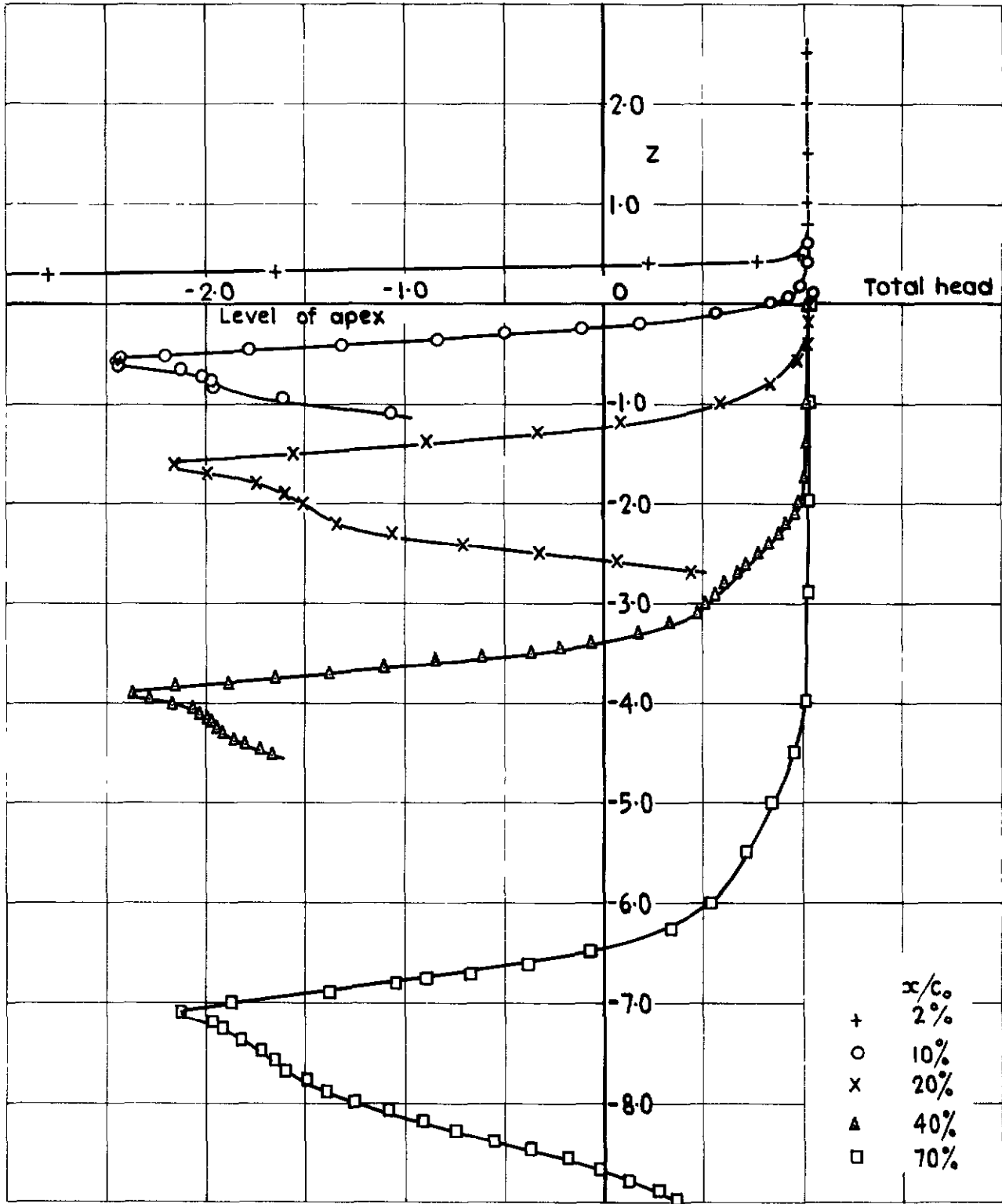


Fig.12 Total head profiles in vertical traverses through vortex centres of wing D at  $\alpha = 16^\circ$



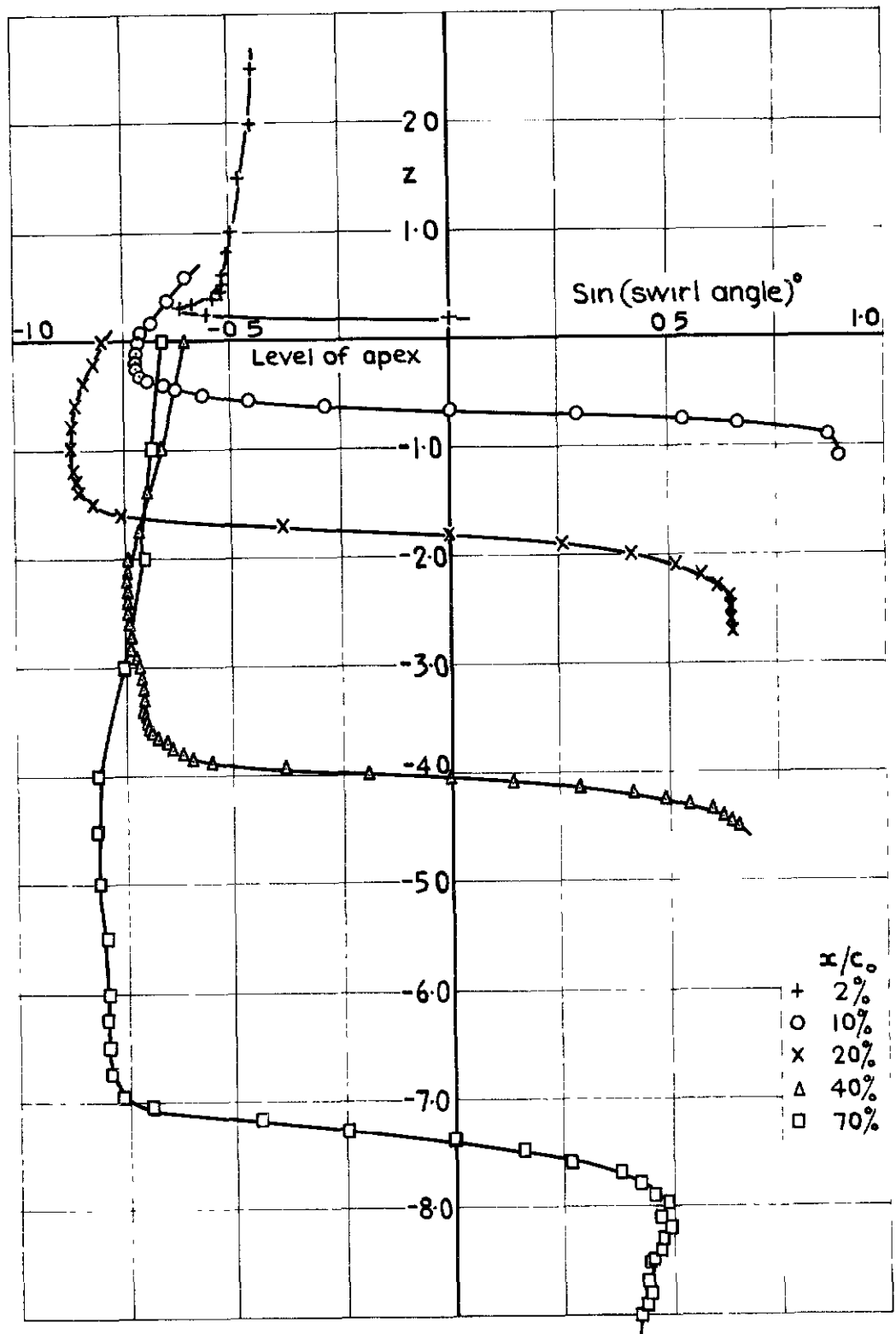


Fig.13 Swirl angle in vertical traverses through vortex centres of wing D at  $\alpha = 16^\circ$

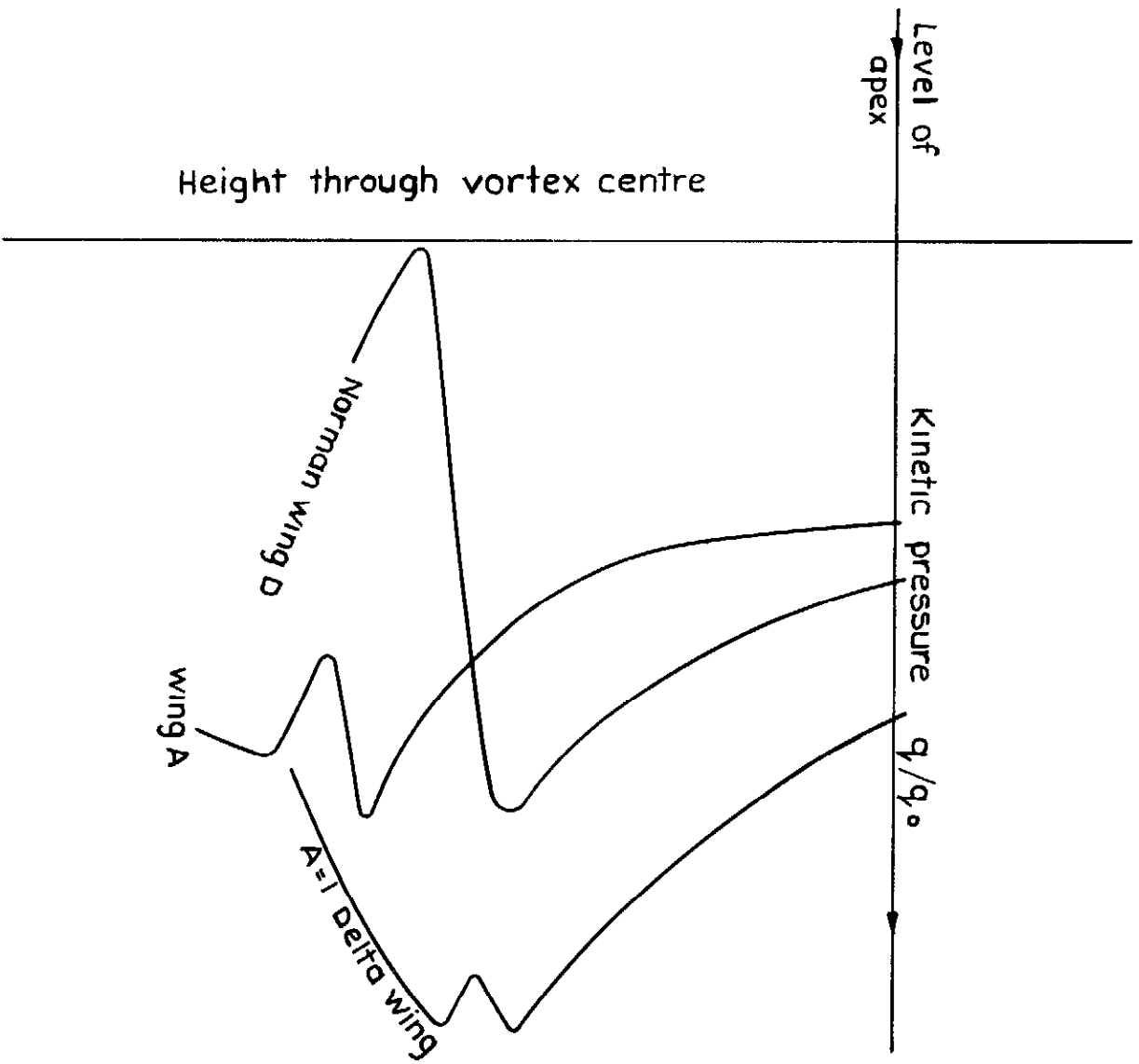


Fig 14 Sketch showing form of kinetic profiles of vortices

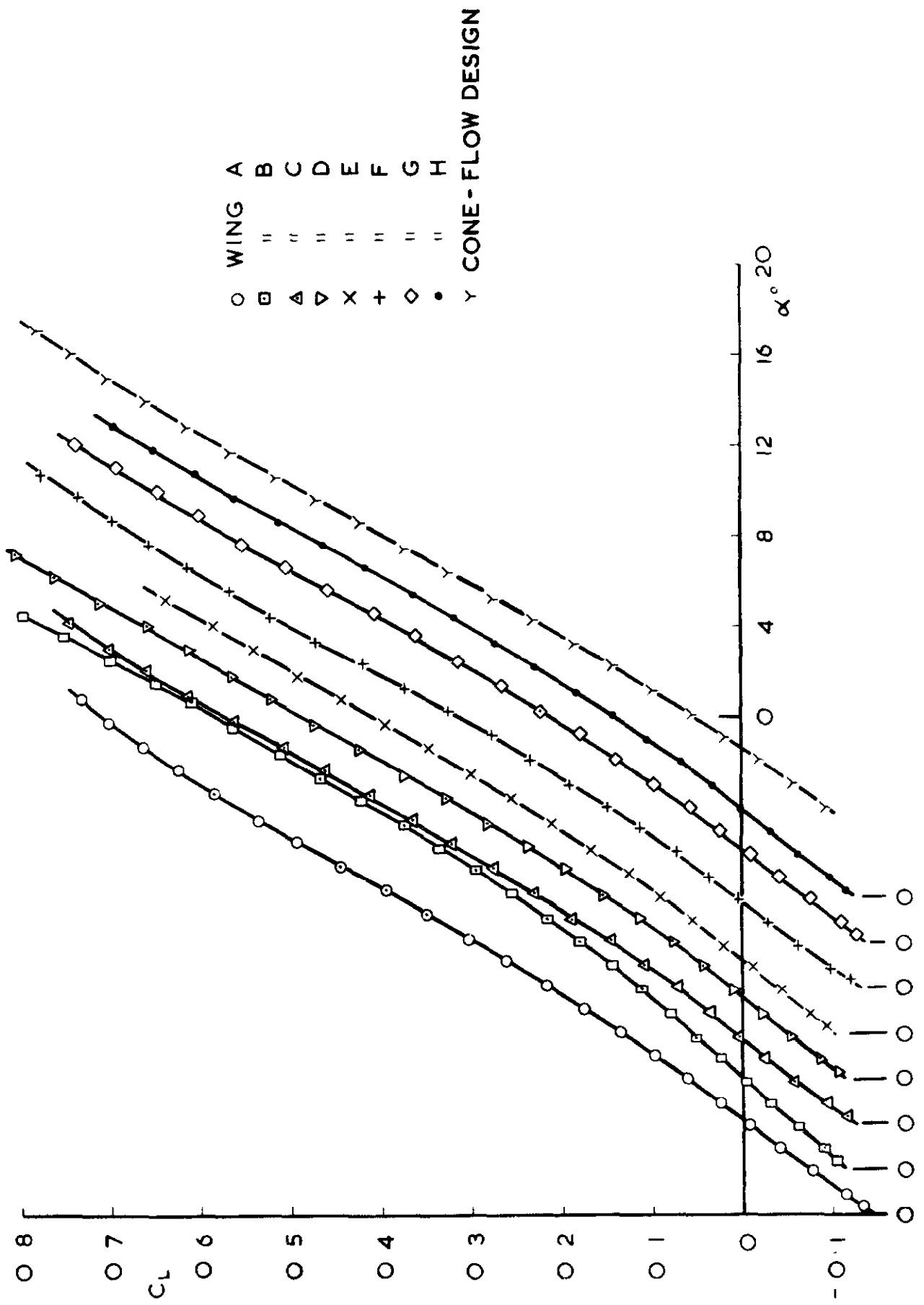


FIG.15 LIFT CURVES OF WAVE-RIDER WINGS

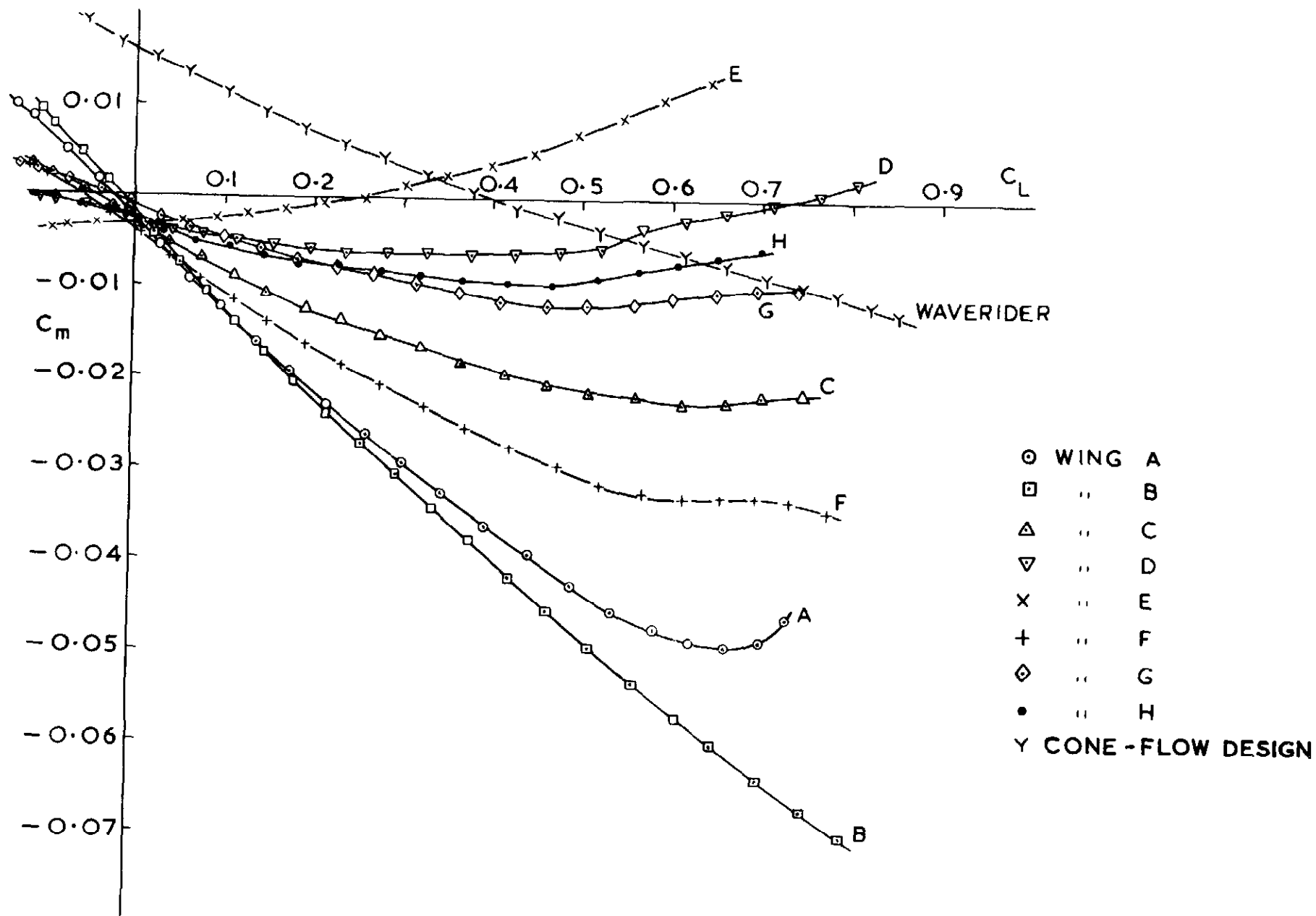


FIG.16 PITCHING MOMENT CURVES OF WAVE-RIDER WINGS

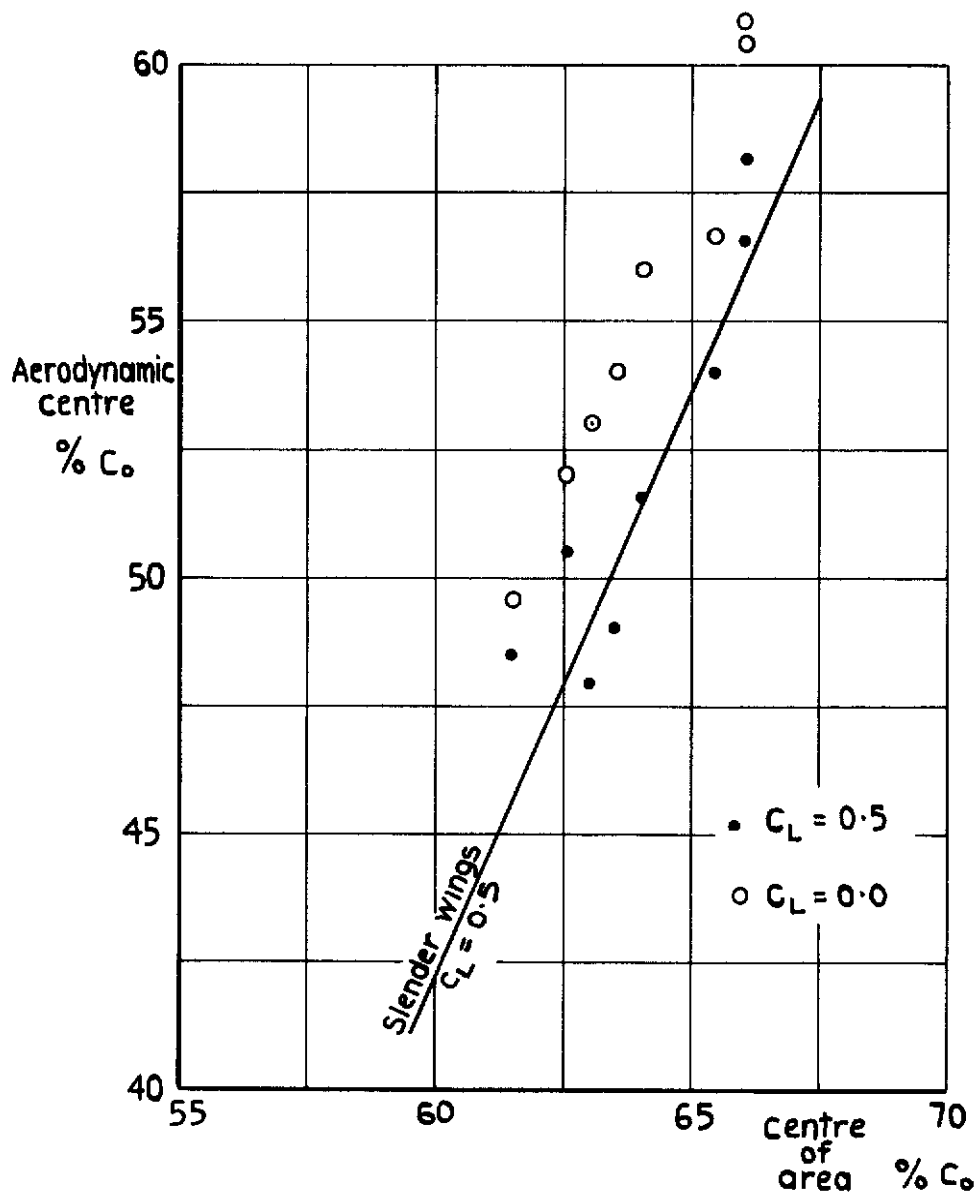


Fig.17 Position of aerodynamic centres of wave-rider wings

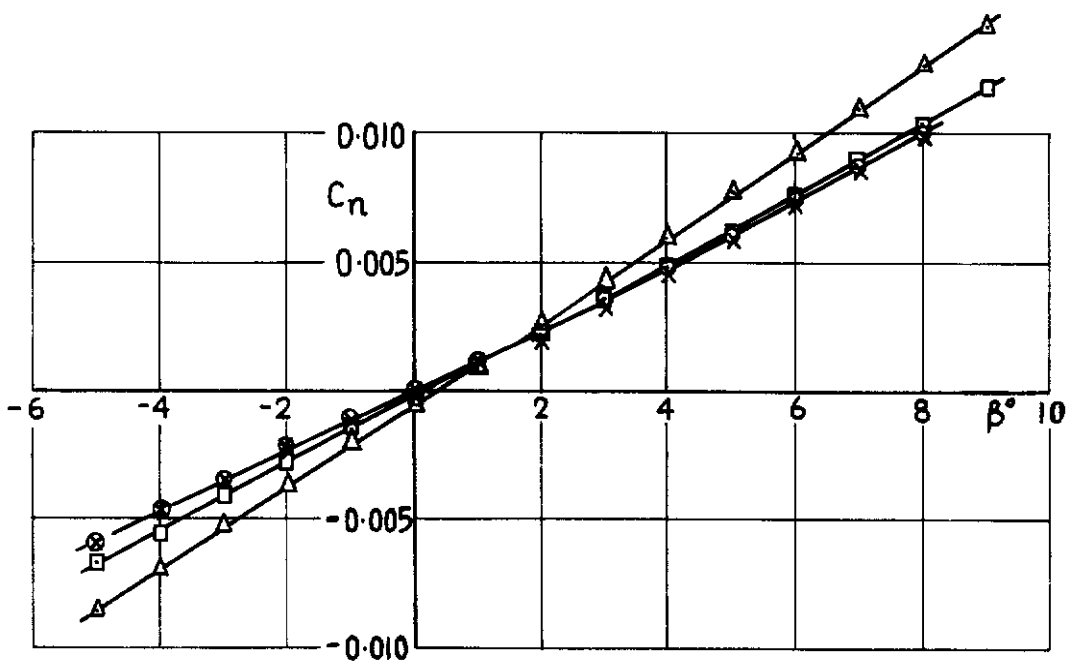
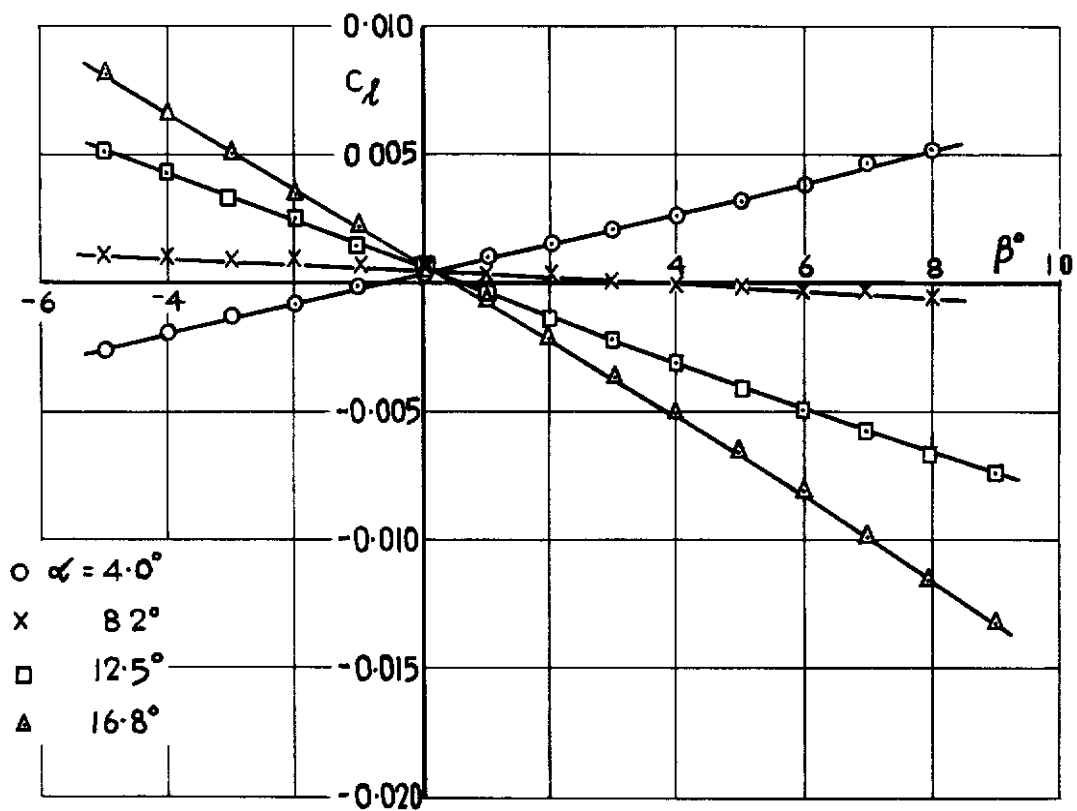


Fig.18 Lateral characteristics of wing D with fin

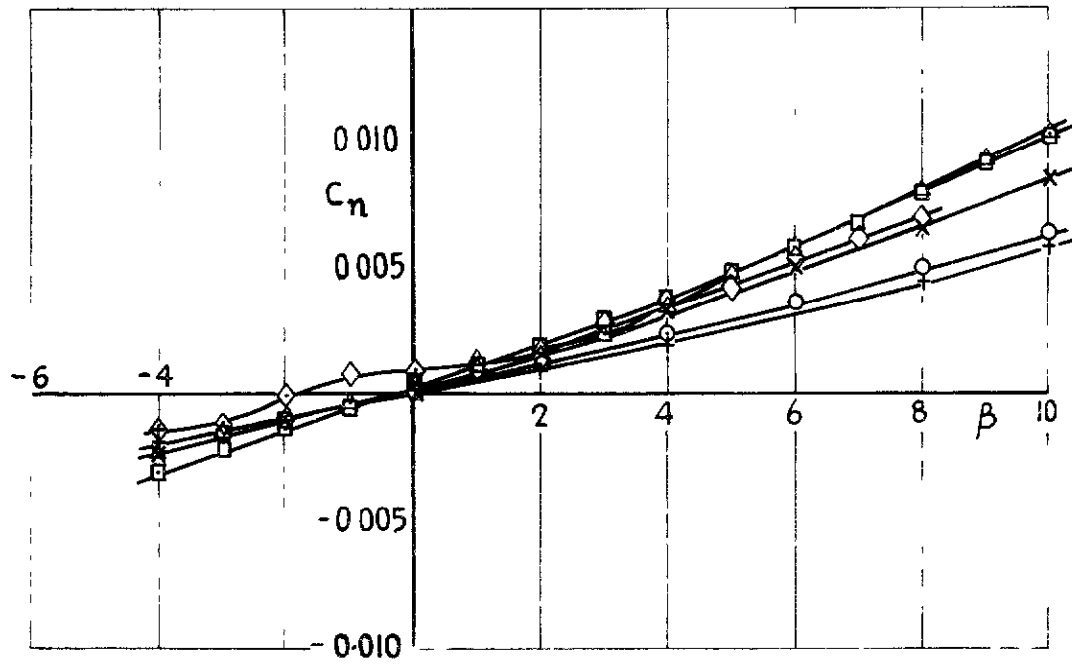
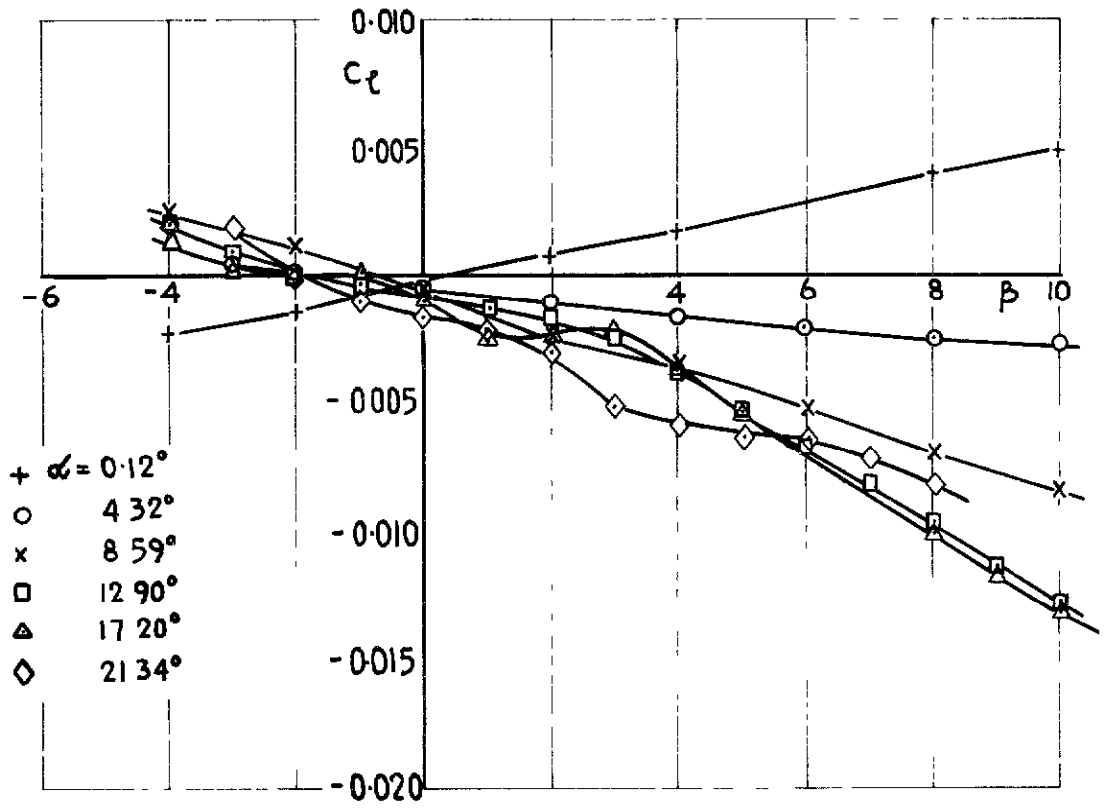


Fig.19 Lateral characteristics of cone-flow wave rider

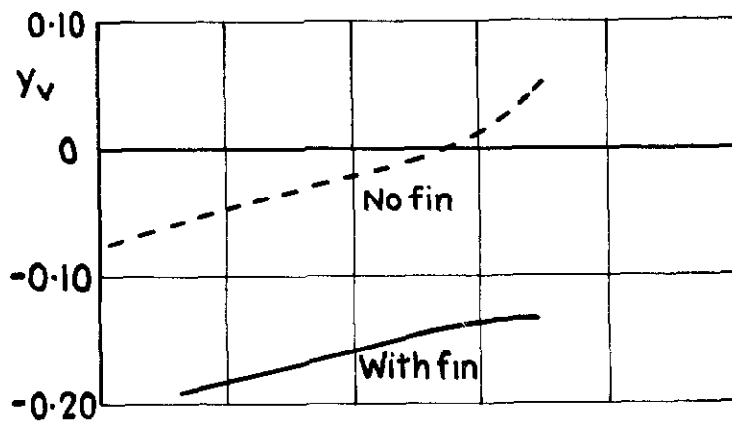
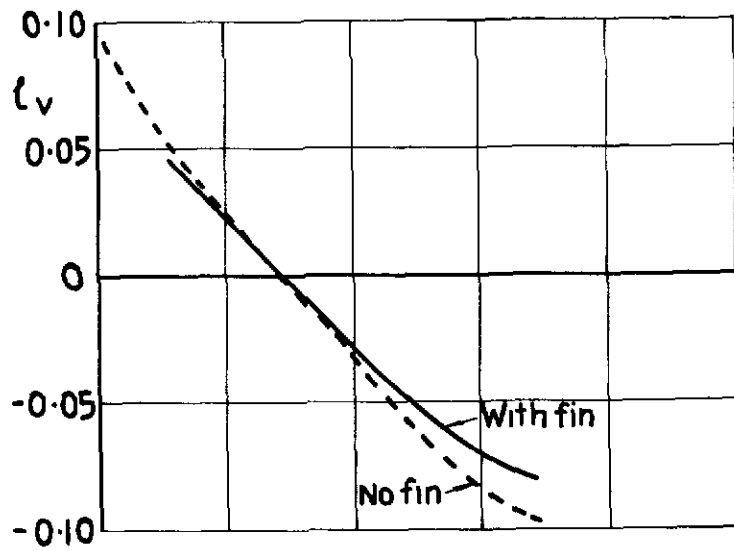
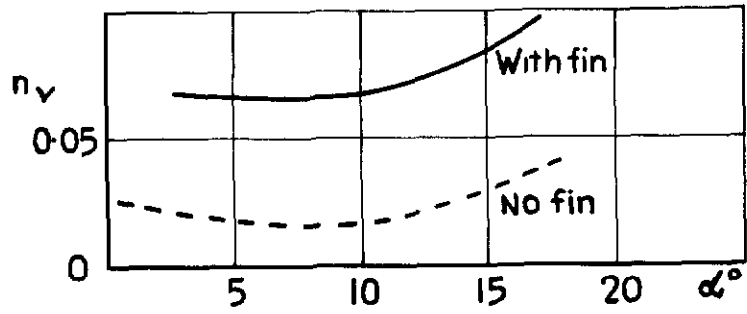


Fig.20 Lateral derivatives of wing D



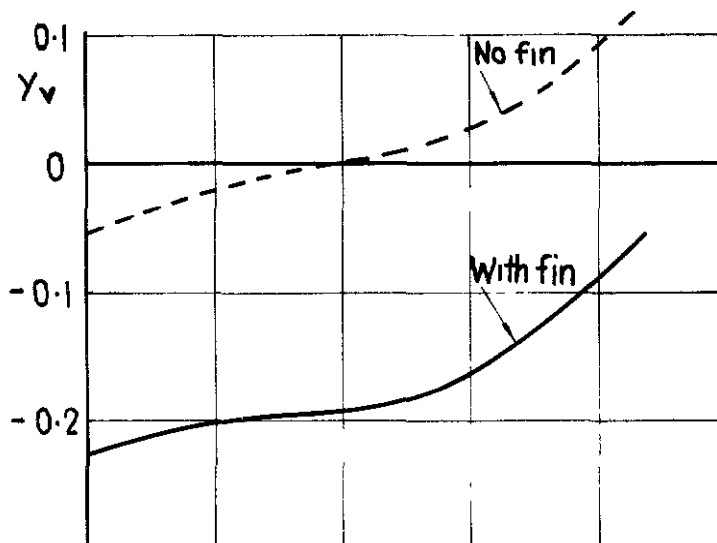
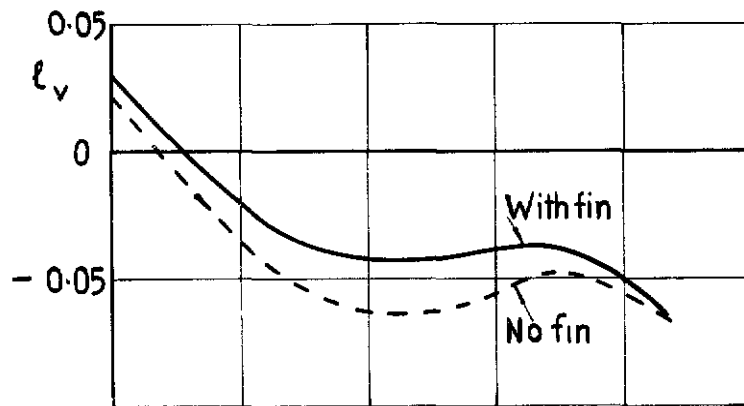
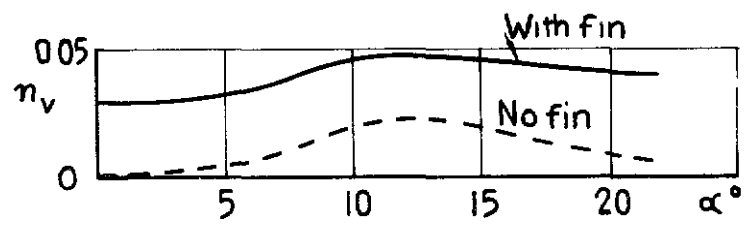


Fig.21 Lateral derivatives of cone-flow wave-rider



A.R.C. C.P. No.1118  
March 1969

Keating, R.F.A.  
Mayne, B.L.

533.692.55 ·  
532.527 ·  
533.6.011.32

#### LOW-SPEED CHARACTERISTICS OF WAVERIDER WINGS

This paper reports on low-speed wind tunnel studies of a series of simple delta-like shapes which might form the basis of future hypersonic aircraft.

The nature of the vortices formed above these wings was investigated by oil-flow experiments, smoke visualisation and flow surveys. Some of the vortices could only be described as broken and had a stagnation point at the centre. Nevertheless, the vortices still had a strong circulation and a high static suction.

The force characteristics were typical of current slender wing designs in spite of the anomalous vortices. The large shift of the aerodynamic

P.T.O.

A.R.C. C.P. No.1118  
March 1969

Keating, R.F.A.  
Mayne, B.L.

533.692.55 :  
532.527 ·  
533.6.011.32

#### LOW-SPEED CHARACTERISTICS OF WAVERIDER WINGS

This paper reports on low-speed wind tunnel studies of a series of simple delta-like shapes which might form the basis of future hypersonic aircraft.

The nature of the vortices formed above these wings was investigated by oil-flow experiments, smoke visualisation and flow surveys. Some of the vortices could only be described as broken and had a stagnation point at the centre. Nevertheless, the vortices still had a strong circulation and a high static suction.

The force characteristics were typical of current slender wing designs in spite of the anomalous vortices. The large shift of the aerodynamic

F.T.O.

A.R.C. C.P. No.1118  
March 1969

Keating, R.F.A.  
Mayne, B.L.

533.692.55 :  
532.527 :  
533.6.011.32

#### LOW-SPEED CHARACTERISTICS OF WAVERIDER WINGS

This paper reports on low-speed wind tunnel studies of a series of simple delta-like shapes which might form the basis of future hypersonic aircraft.

The nature of the vortices formed above these wings was investigated by oil-flow experiments, smoke visualisation and flow surveys. Some of the vortices could only be described as broken and had a stagnation point at the centre. Nevertheless, the vortices still had a strong circulation and a high static suction.

The force characteristics were typical of current slender wing designs in spite of the anomalous vortices. The large shift of the aerodynamic

P.T.O.

centres of the hypersonic planforms when changing from hypersonic to low-speed flight may prove embarrassing.

centres of the hyperbolic planforms when changing from hypersonic to low-speed flight may prove embarrassing.

centres of the hyperbolic planforms when changing from hypersonic to low-speed flight may prove embarrassing.



C.P. No. 1118

© *Crown copyright 1970*

Published by  
HER MAJESTY'S STATIONERY OFFICE

To be purchased from  
49 High Holborn, London w c 1  
13a Castle Street, Edinburgh EH2 3AR  
109 St Mary Street, Cardiff cf1 1jw  
Brazennose Street, Manchester 2  
50 Fairfax Street, Bristol BS1 3DE  
258 Broad Street, Birmingham 1  
7 Linenhall Street, Belfast BT2 8AY  
or through any bookseller

C.P. No. 1118

SBN 11 470318 3